Dynamics of Probe Diffusion in Rod Solutions

Victor Pryamitsyn and Venkat Ganesan

Department of Chemical Engineering, University of Texas at Austin, Austin, Texas 78712, USA

(Received 19 September 2007; published 27 March 2008)

Applications of probe diffusion in polymer matrices typically envision that for particles sizes (R) larger than the correlation length of the polymer solution (ξ), the probe (at long times) diffuses as in a continuum polymer solution. We present simulation results for probe diffusion in rod solutions which challenge this conventional wisdom and indicate a new mechanism of a probe diffusion operative for $R > \xi$. Our simulation results are rationalized by scaling arguments invoking a novel mechanism of the constraint release motion of the rods, and suggest that the dynamical characteristics of the polymer matrix also proves important in developing a complete description of the probe motion.

DOI: 10.1103/PhysRevLett.100.128302 PACS numbers: 83.80.Hj, 47.61.Cb, 83.10.Rs

The diffusional characteristics of tracer particles in crowded solutions of flexible and rigid rod macromolecules prove extremely important for diverse biological phenomena ranging from metabolism, protein-protein interactions, enzyme reactions and gene therapy [1]. Also, many recent experimental developments rely on the diffusional characteristics of colloidal probes to provide information on both the mechanical properties and the structural changes of biological and synthetic macromolecular matrices [2–4].

Of interest in this Letter are the laws that govern the long-time diffusion coefficients of tracer probes in macromolecular matrices. We discuss these issues in the context of the system of spherical probes diffusing in rigid rod solutions which serves as a useful model for many applications. There are three distinct length scales: The size of the probe R, the length of the rods L, and the correlation length of the rod solution ξ (which scales as $c^{-1/2}$, where c denotes the number concentration of the rods [5]). Theories of probe dynamics typically assume that for $R \gtrsim \xi$, the solvent behaves as a continuum fluid and that the probe diffusivity D is inversely proportional to the solution viscosity η_s (''continuum'' picture) [6]. In contrast, for $R \lesssim \xi$ (referred to below as the ''mesh'' picture), a picture of a probe diffusing in a static porous medium of pore size ξ has been used in a variety of hydrodynamic [7], phenomenological [8], and stochastic models [9] to propose functions of the form: $D \propto \exp[-(R/\xi)^{\delta}]/\eta_0$ (η_0 denotes the solvent viscosity) with exponents δ ranging from 0.5–1. In sum, the current theories posit two main modes for probe diffusion with a crossover between them at $R \simeq \xi$.

In this Letter, we use computer simulations and scaling ideas to question the existence of only two dominant modes of diffusion, and whether indeed the length scale governing the crossover to continuum description is the correlation length ξ of the rod solution. Resolution of these issues has several implications. On the one hand, the question of the crossover length scale is critical for the interpretation of experimental tools such as microrheology which are theoretically founded upon a continuum picture [2,3]. Moreover, many of the above-discussed biological applications fall in the regime where $R \simeq \xi$ [10], for which the theoretical descriptions are less well-grounded and in need of possibly new insights.

Computer simulations to probe the above question proves demanding due to the need to account faithfully for (i) the dynamics of the probe, matrix, and the solvent units, (ii) the probe-matrix and matrix-matrix steric interactions at finite concentrations of the matrix, and (iii) the hydrodynamic flows set up by the motion of the particle. In this study, we overcome these challenges by adapting a recently developed explicit solvent simulation approach which combines the ingredients of molecular dynamics and dissipative particle dynamics simulation (DPD) methodologies [11]. In this approach, the solvent particles are represented at a coarse-grained level as spherical units interacting by soft repulsive potentials of the form: $U_{ss} = a/2[1 - r/r_{ss}]^2 (r < r_{ss})$, where a and r_{ss} represent, respectively, the strength and range of interaction. In contrast, the rod particles are represented by a string of spherical monomers linked in a ''shish-kebab'' model, interacting pairwise by steeply repulsive Lennard-Jones (LJ) potentials truncated at the attractive upturn (the location of which was fixed at r_{ss}). The probe is also modeled as a spherical particle interacting with the rod monomers and the solvent units by repulsive LJ potentials truncated at the attractive upturn. The rod-solvent interactions are chosen to be identical to the solvent-solvent interactions [12]. To incorporate hydrodynamical phenomena, we retain the original DPD approach [13], which incorporates momentum conserving velocity dependent forces (between rod-solvent, probe-solvent, and solvent-solvent units) along the line of centers of the interacting particles.

In a recent article we used the above simulation approach to study dynamics and rheology of rod solutions from dilute to concentrated regimes and demonstrated excellent agreement with the corresponding theoretical predictions [14]. For the present research, we studied the dynamics of probes of sizes $R = 2$, 3, 5, 6, 7, and 8 in rod solutions of lengths $L = 10$, 15, and 20 (all lengths non-

dimensionalized by r_{ss}) at concentrations $0.7 \lesssim cL^3 \lesssim 85$ which places our simulations in the regime $0.3 < R/\xi < 20$ [15]—i.e. predominantly in the regime wherein the continuum picture is expected to be applicable. Other numerical details and interaction parameters adopted in this study are identical to those used in our earlier article [14]. We determined sedimentation coefficients by applying a small drag force to the tracer probe and calculated its average drift velocity v_d in the direction of applied force f_d. The diffusion coefficient of the probe was then extracted using the fluctuation-dissipation theorem (FDT) as: $D = f_d/v_d$ (units of k_BT) [16]. The simulations were typically repeated for different drag forces to verify the linearity of the force-velocity relationship.

In Fig. 1 we display the normalized probe diffusivities D and the inverse of the solvent viscosities η_s as functions of cL^3 for a number of different pairs of probe sizes R and rod lengths L. As expected from theories for rheology of rod suspensions, η_s/η_0 displays a very good collapse as a function of cL^3 [5] (minor deviations can be attributed to the role of hydrodynamic interactions [14]). If the continuum picture were applicable for probe diffusion, we expect $D/D_0 \propto \eta_0/\eta_s$. In contrast, we observe that D/D_0 is a function of both R and L (in addition to cL^3) and is also consistently higher η_0/η_s.

At first sight, the results presented in Fig. 1 appear qualitatively consistent with the trends discussed in the introduction. Indeed, small probe sizes may be in the mesh regime of probe diffusion for which long-time diffusivities are expected to be much greater than the continuum values. In contrast, as observed for $R = 7$ and 8, larger probes do show a trend approaching continuum regime which corresponds to the behavior expected for $R/\xi \gtrsim 1$. To examine this issue more carefully, in

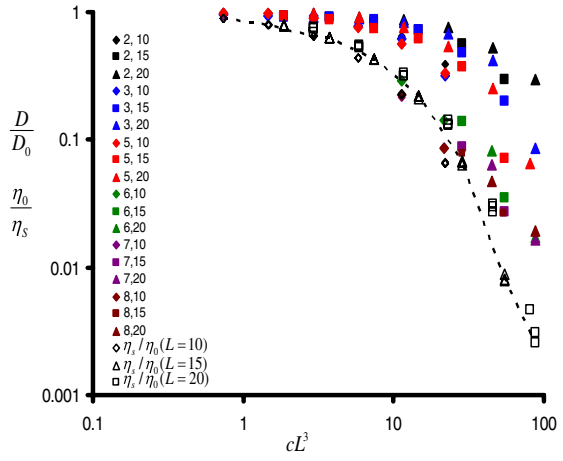

FIG. 1 (color online). Rod concentration (expressed as cL^3) dependencies of the probe diffusivities D (for different R, L pairs indicated) normalized by its value in the pure solvent medium D_0, and the inverse suspension viscosities η_s normalized by the solvent viscosity η_0 (open symbols) for rod suspensions [14]. The dotted line is a guide line depicting the concentration dependencies of the inverse suspension viscosities.

Figs. 2(a) and 2(b), we display the values of D/D_0 and $D\eta_s/D_0\eta_0$ as explicit functions of R/ξ. Consistent with the mesh regime, it is seen in Fig. 2(a) that for the (limited) results in the regime $R/\xi \lesssim 1$ the D/D_0 values for the different radii does appear to approach a universal function (albeit, lack of numerical resolution precludes a definitive conclusion). However, Fig. 2(b) suggests a more profound result that for $R/\xi \gtrsim 1$ our simulation results do not approach the trend consistent with the continuum expectation that $D\eta_s/D_0\eta_0 \simeq$ constant. This result raises the question whether the mode of diffusion switches to the continuum picture for $R \gtrsim \xi$, or whether a different mechanism becomes operative after the mesh regime.

We note that microrheology experiments in the continuum regime have also observed deviations between probe diffusivities and the macroscopic solution viscosities, and have attributed them to the presence of a ''depletion'' zone around the probe with rheological characteristics different from that of the bulk solution [2,17]. To examine whether such effects can explain the deviations in Fig. 1, we probed the local density distribution of the rod monomers around the test particle. We then used such results in a shell model [17] envisioning the motion of the probe as that of a particle surrounded by a layer with solvent viscosity η_0 moving as a composite particle in a solution of viscosity η_s [18]. Representative results of such predictions are displayed Figs. 3(a) and 3(b) where it is seen that while the depletion effects do enhance the expected values of probe diffusivities in the continuum picture, they still do not

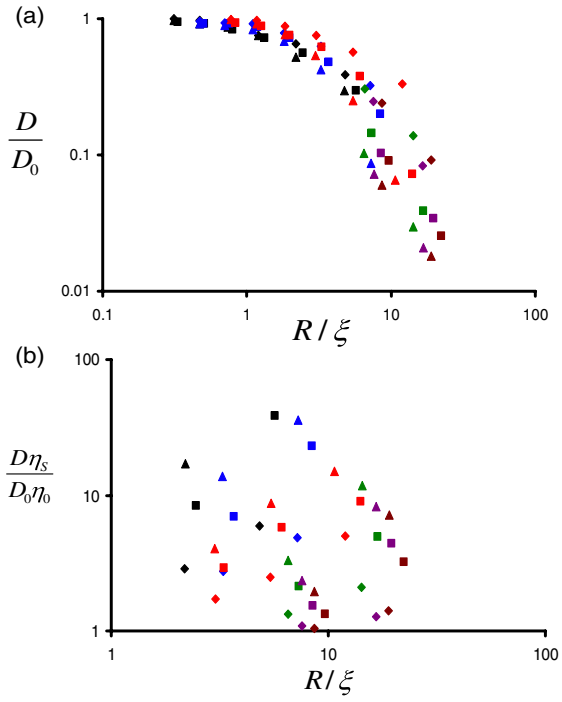

FIG. 2 (color online). (The symbol legends are identical to Fig. 1.) Probe diffusivities D normalized by: (a) D_0; (b) $D_0\eta_0/\eta_S$, and displayed as a function R/ξ. (b) displays only results corresponding to $R/\xi > 2$.

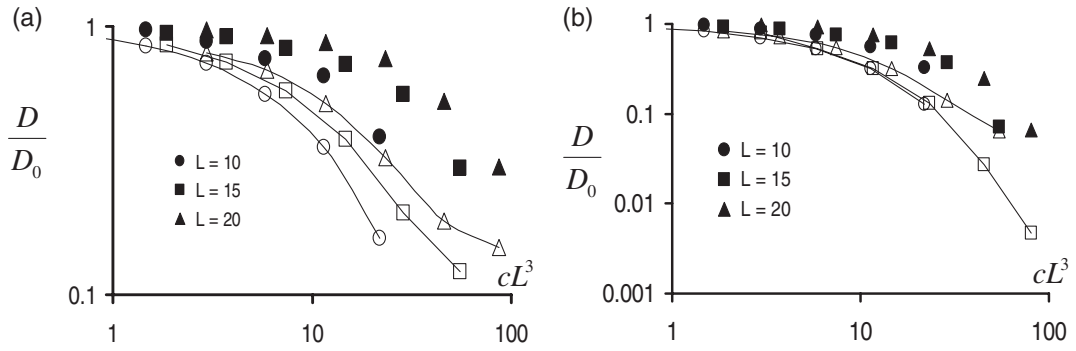

FIG. 3. A comparison of our simulation results (closed, unconnected symbols) with the predictions of the probe diffusivity (connected open symbols) based on the shell model of Tuinier [17]: (a) $R = 2$; (b) $R = 5$.

suffice to explain our simulation results. In turn, this demonstration confirms that our simulation results are not a manifestation of the continuum regime of probe diffusion.

To rationalize our results, we suggest a mechanism of constraint release (CR) motion of the spherical probes for entangled rodlike solutions. We point out the analogy between the motion of the probe in the matrix and the motion of a long tracer polymer in a matrix of shorter entangled polymers. In the latter instance, the longer polymer has the same option of dragging the shorter polymers with it as it moves, which in turn would lead to the classical continuum prediction of a Stokes diffusivity. Alternatively, the longer polymer may move (a tube diameter) when one of its entanglements with the shorter polymers is released due to the reptation of the shorter polymer. These two mechanisms operate simultaneously in a competitive manner such that the effective tracer diffusivity is determined by the mechanism which dominates [19]. We believe that a similar scenario accompanies the motion of a spherical probe for $R > \xi$. In such a regime the probe is trapped in the mesh of rods, and the scenario of the particle dragging the rods is equivalent to that embodied in the continuum picture and leads to a diffusivity which scales as η_s^{-1} (except insofar as possible depletion effects). Alternatively, the translational diffusion of a constraining (entangled) rod may release and thereby open up a new space for the probe to occupy. Successive constraint release events may thereby facilitate diffusion over longer time scales [Figs. 4(a) and 4(b)].

We estimate the time and length scales accompanying the constraint release motions of the probe in entangled rod solutions [cf. Fig. 4(c)]. If we consider a hypothetical one dimensional motion of the probe, over a length Δ, the number of potential obstacles to its motion can be estimated as: $n_R \sim cR(R + L)\Delta$. The average distance between the obstacles λ can then be estimated as $\lambda \sim \Delta/n_R = [R(R + L)c]^{-1}$. λ represents an estimate for the step size for the particle's random motion arising from the constraint release mechanism. If we now consider a specific obstacle (rod) blocking the motion of the probe, an estimate of the survival time scale of this obstacle is $\tau \propto (R + L)^2/D_{\|}$, where $D_{\|}$ denotes the translational diffusion coefficient of the rods parallel to its own axis (the perpendicular component of D is expected to be negligible in entangled solutions). Using the above, we obtain an estimate for the constraint release probe diffusivity as

$$D_{\text{cons}} \propto \frac{\lambda^2}{\tau} = \frac{D_{\|}}{\alpha^2(\alpha + 1)^4(cL^3)^2}, \tag{1}$$

where $\alpha = R/L$. Explicitly, D_{cons} is expected to scale R^{-2} and $(cL^3)^{-2}$ (for $R \ll L$) in contrast to the R^{-1} and η_s^{-1} [which in turn scales as $(cL^3)^3$ [5]] scaling expected for the Stokes-Einstein (SE) regime.

In Fig. 5 we display our simulation results for D/D_0 as a function of the parameter suggested by the above scaling Eq. (1). We observe that in this representation, our diffusivity results for all the probe radii and matrix conditions show a very good collapse into a single universal functional form which asymptotically approaches the dependence predicted above. Considering the approximate nature of our scaling estimates, this scaling collapse dem-

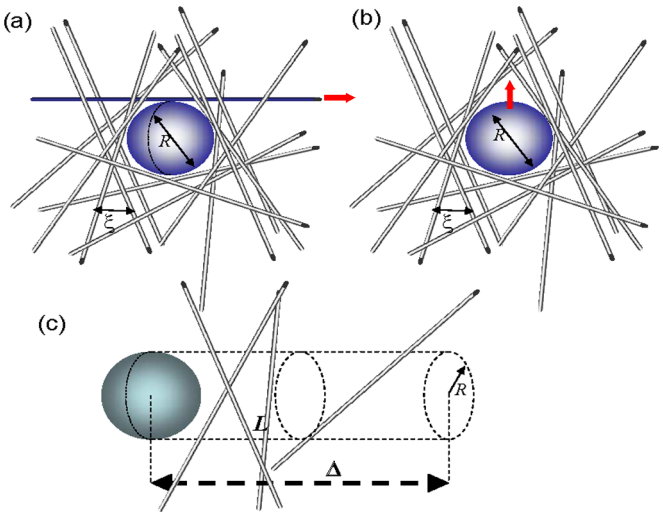

FIG. 4 (color online). (a) and (b) A schematic of the mechanism of constraint release for probes entangled in the mesh. Translational diffusion of the shaded rod opens up space for the particle to diffuse into; (c) a schematic illustrating the construction of our scaling idea.

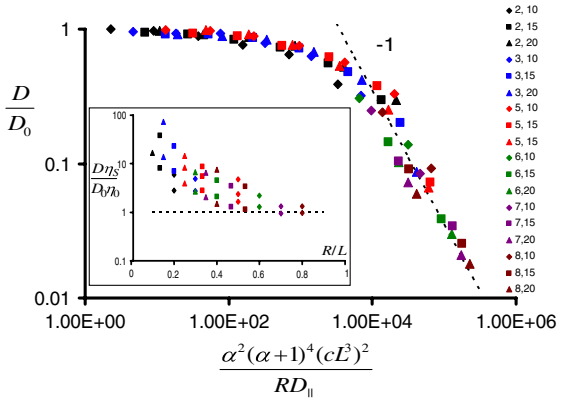

FIG. 5 (color online). A test of the scaling prediction [Eq. (1)] underlying the CR mechanism. The points are our simulation results for the diffusivities for different R, L combinations indicated ($D_{\|}$ values were obtained in our earlier study [14]). The dashed line represents the slope of -1 predicted in our model. The inset displays the data of Fig. 2(b) as a function of R/L.

onstration serves as a strong validation of our hypothesis that the CR mechanism rationalizes the simulation results for probe diffusion.

It is of interest to compare the prediction of Eq. (1) with the SE mechanism to determine if there is ever a crossover from CR to the SE mechanism. If we compare (1) with the SE prediction $D/D_0 \propto \eta_s^{-1}$ [using the asymptotic scaling $\eta_s \propto (cL^3)^3$ [5]], we obtain a dominance of the SE mechanism for $R > L(cL^3)^{1/5}$. This estimate for crossover neglects the effects arising from the depletion of rods, which as demonstrated in Fig. 3(b) would lead to a faster diffusion than assumed in the SE mechanism. In combination with the small value of the exponent of cL^3, in experimental situations we expect the crossover to the continuum picture occur at approximately $R \simeq L$. This expectation is consistent with the approach to the continuum prediction seen for larger probe sizes in Fig. 1. More clearly, in the inset to Fig. 5 we depict the results of Fig. 2(b) as a function of R/L and observe an asymptotic approach to the continuum limit for $R/L \simeq O(1)$ [20].

In conclusion, we have presented simulation evidence for a new mode of transport of probe particles in rodlike suspensions. This mechanism is expected to be operative for the situation when the particle size $\xi \lesssim R \lesssim L$ and postulates a constraint release motion of the rods aiding the diffusion of the particles. This mechanism is shown by scaling arguments and simulation results to lead to a nontrivial dependence of the diffusivity upon the particle size R and the concentration of the rod suspension c. Overall, our results and the arguments presented challenge conventional wisdom that the crossover to continuum regime of probe motion occurs when the radius of the particle becomes larger than the correlation length of the solution. In contrast, we suggest that accounting for the dynamical characteristics of the matrix proves critical in developing a complete description of the particle motion. This conclusion is expected to have ramifications for a wide range of applications and experimental tools which rely on the diffusional characteristics of probes in macromolecular solutions.

This work was supported in part by a grant from Robert A. Welch Foundation and the U.S. Army Research Office under Grant No. W911NF-07-1-0268. The simulations used computers at Texas Advanced Computing Center.

[1] T. Pederson, Nat. Cell Biol. **2**, E73 (2000).
[2] D. T. Chen *et al.*, Phys. Rev. Lett. **90**, 108301 (2003).
[3] A. J. Levine and T. C. Lubensky, Phys. Rev. Lett. **85**, 1774 (2000).
[4] I. Golding and E. C. Cox, Phys. Rev. Lett. **96**, 098102 (2006); M. T. Valentine *et al.*, Biophys. J. **88**, 680 (2005).
[5] M. Doi and S. Edwards, *The Theory of Polymer Dynamics* (Oxford University Press, New York, 1986).
[6] A. Einstein, *Investigations on the Theory of the Brownian Movement* (Courier Dover Publications, New York, 1956).
[7] R. I. Cukier, Macromolecules **17**, 252 (1984).
[8] B. Amsden, Macromolecules **31**, 8382 (1998).
[9] A. Ogston, B. Preston, and J. Wells, Proc. R. Soc. A **333**, 297 (1973).
[10] J. D. Jones and K. Luby-Phelps, Biophys. J. **71**, 2742 (1996); K. Luby-Phelps, Curr. Opin. Cell Biol. **6**, 3 (1994).
[11] V. Pryamitsyn and V. Ganesan, J. Chem. Phys. **122**, 104906 (2005).
[12] In conjunction with the soft nature of solvent-solvent interactions, the latter parametrization eliminates spurious depletion induced attractions between the rod units as well as the rod units and the probe.
[13] R. D. Groot and P. B. Warren, J. Chem. Phys. **107**, 4423 (1997).
[14] V. Pryamitsyn and V. Ganesan, J. Chem. Phys. (to be published).
[15] ξ is estimated as the average pore size in a rod suspension at a given rod concentration. The distribution of pore sizes in rod suspensions have been computed in A. G. Ogston, Trans. Faraday Soc. **54**, 1754 (1958).
[16] Validity of FDT was tested explicitly for regimes in the lower concentrations of rods.
[17] T. H. Fan, J. K. G. Dhont, and R. Tuinier, Phys. Rev. E **75**, 011803 (2007); R. Tuinier, J. K. G. Dhont, and T. H. Fan, Europhys. Lett. **75**, 929 (2006); G. H. Koenderink *et al.*, Phys. Rev. E **69**, 021804 (2004).
[18] The assumption of the solvent viscosity for the shell is expected to render such predictions as an upper bound for the influence of depletion layers upon the probe diffusivity.
[19] F. Brochard-Wyart *et al.*, Macromolecules **27**, 803 (1994).
[20] Because of computational limitations we were unable to probe the dynamics of much larger particles.